MODELING OF MORPHOLOGICAL DEVELOPMENT IN POLYIMIDE MICROSPHERES OBTAINED FROM POWDERED PRECURSORS

Camilo I. Cano, Ph.D and R. Byron Pipes, Ph.D, NAE, IVA
School of Chemical Engineering, Purdue University, West Lafayette, IN

Abstract

The synthesis of high performance polyimide foams by the solid-state powder foaming of poly(amic acid) powders, containing hydrogen bonded blowing agent (THF), is described. During the thermal inflation of poly(amic acid) particles into polyimide microspheres, their fusion has been shown to produce the desired cellular architecture.

In the present work, the solid state powder foaming process is modeled by studying the concurrent phenomena such as transport processes and polymerization reactions in a single particle of spherical geometry and imposing the appropriate initial and boundary conditions. The simulation of the inflation process spans from poly(amic acid) particles to polyimide microstructures and the rheological and diffusional properties of the evolving polymer are related to its molecular changes (increase in molecular weight and cyclization) and loss of dissolved blowing agent. Morphological aspects of the initial precursor particles, as well as, plastization effects by the reaction solvents are found to be determinant parameters in the inflation process and determine the ultimate size of the resulting polyimide microspheres.

Introduction

Application of polyimides as high performance polymers ranges from films to specialized cellular materials. Cellular materials in particular have received special attention recently due to increased demands for resistant thermal and acoustic insulation. In this work, numerical simulation of a novel method for preparing foams based on powdered precursors [1] is presented. This method consists on the inflation of microscopic pre-polymer (poly (amic acid)) particles which contain solvents (methanol and THF) that act as blowing agents [2, 3]. Upon temperature increase, the particles inflate to become microspheres with different dimensions and morphological variations (Figure 1). The presence of multiple particles inside a mold allows bubble impingement and fusion and yields a neat foamed article.
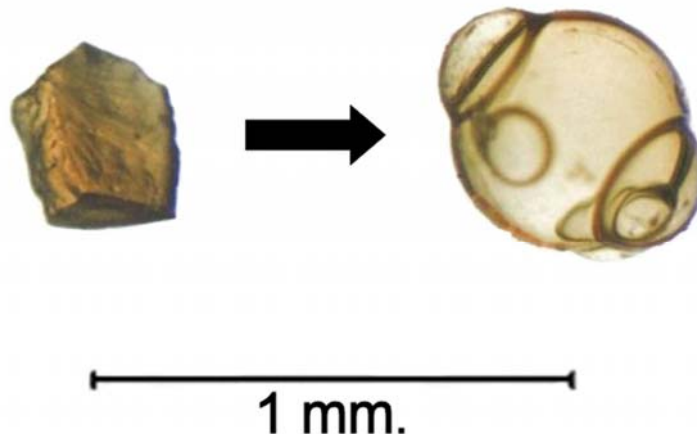

Figure 1. Micrographs showing particle inflation into microstructure upon temperature increase.

Previously it has been shown that one of the primary phenomena related to the inflation of these precursors is the competitive diffusion of solvent within the particle and towards the outside of the particle [2, 3]. Additionally, other parameters of importance are the precursor particle morphology (internal features, size and shape) [2] (Figure 2), as well as the development of molecular structure due to amidation and imidization reactions that occur concurrently to particle inflation [4].
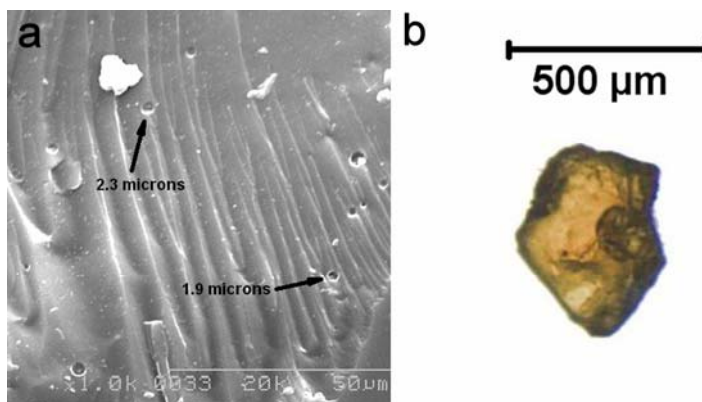

Figure 2. Electron and optical micrographs evidencing different void sizes that act as bubble growth sites in the particles: a. microvoids (0.5 μm – 5 μm), b. macrovoids (50 – 100 μm).

The complexity of analyzing the different simultaneous phenomena and the need to accurately predict the morphology of final structures as a function of processing parameters has motivated the development of a numerical approach. In the present paper this first-principle numerical model is presented and a parametric study is performed to determine the effect of the different variables and parameters in the solid state powder foaming process.

Numerical Model Development

Numerical modeling of the solid state powder foaming process has been divided in two separate stages. The first stage deals with all the phenomena that occur from the initiation of heating to the onset of particle inflation. The second stage describes the process of particle inflation and is presented in the present work. The reader is referred to other pieces of work by the authors where the first stage is described [4, 5].

A common polyimide system was chosen for the present analysis. Properties for the polyimide made from reacting 3,3′,4,4′-benzophenonetetracarboxylic dianhydride (BTDA) and 4,4′-oxydianiline (4,4′-ODA)were employed. Methanol and Tetrahydrofuran (THF) acted as the reaction solvents and primary blowing agents [2].

For the present model a spherical particle (radius S), composed of poly(amic acid) precursor and dissolved blowing agent, with a pre-existing concentric spherical void (radius R) is assumed (Figure 3 inset). The beginning of the present analysis corresponds to the second stage mentioned above and as such is expected to start during the process temperature increase and in the vicinity of the effective glass transition temperature, T_g, of the precursor material. At this point, the pressure inside the nucleus is sufficient to overcome the hydrodynamic restrictions of the precursor solution and inflation begins. Enhanced mobility favors the onset of amidation reactions which slowly increase the molecular weight, as well as imidization reactions which increase the T_g of the material. The combined effect of devolatilization, molecular weight increase and imidization contribute to the cessation of bubble growth. As can be expected, these concurrent processes affect the material properties of the precursor. These property changes can be followed effectively by means of the T_g. The following expression allows calculation of the effect of solvent plastization on the polymer [6]:

$$T_g = \frac{\Delta\alpha_s T_{g,s} w_s + \Delta\alpha_P T_{g,P} w_P}{\Delta\alpha_s w_s + \Delta\alpha_P w_P} + \frac{\Delta k \, w_s w_P}{\Delta\alpha_s w_s + \Delta\alpha_P w_P} \tag{1}$$

where $\Delta\alpha$ is the difference between the volume expansion coefficients of solvent S and polymer P in the rubbery (or liquid) and glassy states and w is the weight fraction. The parameter Δk represents the excess volume change of mixing for the two components.

The effect of molecular structure change is expressed in terms of the so-called Fox-equation:

$$\frac{1}{T_g} = \frac{w_{PAA}}{T_{g,PAA}} + \frac{w_{PI}}{T_{g,PI}} \tag{2}$$

where w_{PAA} and w_{PI} stand for the weight fractions of PAA and polyimide repeat units, respectively. This equation calculates the effective T_g of the copolymer from the T_g of the two components (PAA and polyimide) assuming a random copolymer exists during the imidization process. For the sake of document briefness, the determination and estimation procedure for the different material and transport properties (e.g. viscosity, diffusivity, etc.) as a function of molecular structure, temperature and solvent concentration can be found elsewhere [3].

Analysis of the inflation process requires that the transport processes within the particles be studied. The present numerical scenario can be explained as the growth of a polymeric spherical shell. This problem is similar to that approached by Arefmanesh et al [7] except the fact that the present model's boundary condition corresponds to a physical boundary at the surface of the particle. At this boundary the concentration becomes zero and the temperature is that of the surrounding environment. The governing expressions for the model's geometry are:

$$\frac{\partial C}{\partial t} = 9D \frac{\partial}{\partial y}\left(\left(y + R^3\right)^{\frac{4}{3}} \frac{\partial C}{\partial y} \right) + V_a \tag{3}$$

$$\frac{\partial T}{\partial t} = 9D_T \frac{\partial}{\partial y}\left(\left(y + R^3\right)^{\frac{4}{3}} \frac{\partial T}{\partial y} \right) + Q_a \tag{4}$$

where, T is the absolute temperature, C is the concentration of volatiles expressed as mass fraction, t is the time coordinate, D is the mass diffusion coefficient, D_T is the thermal diffusivity, R is the radius of the growing bubble (nucleus), V_a is a mass generation term for volatiles formed from the condensation reactions, Q_a is a heat generation term and y is a transformed spatial coordinate defined as:

$$y = r^3 - R^3(t) \tag{5}$$

The initial and boundary conditions for the mass and thermal diffusion equations are:

$$C(y,0) = C_{Tg}(y) \quad \text{and} \quad T(y,0) = T_{Tg}(y)$$

$$C(0,t) = \frac{P_g}{H_c} \quad \text{and} \quad C(S^3 - R^3, t) = 0$$

$$\left.\frac{\partial T}{\partial y}\right|_{y=0} = 0 \quad \text{and} \quad T(S^3 - R^3, t) = T_\infty$$

where $C_{Tg}(y)$ and $T_{Tg}(y)$ are the concentration and temperature profiles at the end of the first stage. The numerical procedure for the determination of such conditions is presented in detail elsewhere [4, 5]. P_g is the pressure of the volatiles inside the growing bubble and H_c is the weight fraction-based Henry's constant defined as:

$$H_c = P_v(v_1/v_2)\exp(1+\chi) \tag{6}$$

where v_1 and v_2 are the specific volumes of volatile component and polymer respectively, P_v is the vapor pressure of the pure volatile component, and χ is the Flory-Huggins interaction parameter. T_∞ is the ambient temperature surrounding the particles, which for this analysis varies linearly with time (at a constant heating rate, m) according to:

$$T_\infty = T_0 + m \cdot t \tag{7}$$

Simultaneously with the inflation process, the non-isothermal conditions of the process allow for enhanced reactivity of the precursor which leads to amidation and, at higher temperatures, imidization reactions. Both reactions produce condensation byproducts (methanol and water, respectively). The fact that THF, which is the reaction solvent, exists in much more quantity than the other two volatiles (i.e. methanol and water), allows the simplifying assumption that there is only a single volatile component that acts as blowing agent (BA) (i.e. THF). The mass and heat generation terms in Equations (3) and (4) account for the generation of additional BA in form of the condensation byproducts (also referred to as secondary blowing agent), as well as for the endothermic requirement of both reactions. These generation terms are described as:

$$V_a = \frac{M_a}{M_T}\left(\frac{d\alpha_a}{dT}\right)\left(\frac{dT}{dt}\right) + \frac{M_i}{M_T}\left(\frac{d\alpha_i}{dT}\right)\left(\frac{dT}{dt}\right) \tag{8}$$

$$Q_a = \frac{1}{C_P}\left[\begin{array}{l}\Delta H_{RA}\left(\frac{M_{Mon}}{M_T}\right)\left(\frac{d\alpha_a}{dT}\right)\left(\frac{dT}{dt}\right) + \\ \Delta H_{RI}\left(\frac{M_{PAA}}{M_T}\right)\left(\frac{d\alpha_i}{dT}\right)\left(\frac{dT}{dt}\right)\end{array}\right] \tag{9}$$

where α_a and α_i refer to the degrees of conversion of the amidation and imidization reactions, M_a and M_i are the stoichiometric mass quantities of volatiles produced during the amidation and imidization, ΔH_{RA} and ΔH_{RI} are the heat of reaction absorbed by the amidation and imidization reactions (Table 1) and M_{mon}, and M_{PAA} refer to the mass of monomeric and amic-acid groups that react, respectively. M_T is the particle mass introduced to normalize V_a and Q_a in terms of weight fraction concentration. The general differential expression used to relate non-isothermal conversion is:

$$\frac{d\alpha}{dT} = \frac{A}{m}\exp\left(\frac{-E_a}{RT}\right)(1-\alpha)^n \tag{10}$$

where n is the order of the reaction (i.e. n = 2 for the imidization and n = 1 for the amidation) [4], A and Ea are the frequency factor and activation energies of each reaction, respectively, and m is the heating rate. The specific kinetic parameters obtained experimentally for these reactions are summarized in Table 1.

The growth of the bubble inside the spherical shell can be described by:

$$P_{atm} - P_g + 2\gamma\left(\frac{1}{S} + \frac{1}{R}\right) - 4\eta R^2 \dot{R}\left(\frac{1}{S^3} - \frac{1}{R^3}\right) = 0 \tag{11}$$

The gas pressure responsible for the bubble growth within the shell responds t changes in temperature, volume and mass whithin the bubble. The mass change comes from the diffusion of volatiles both in and out of the bubble through the polymer-bubble interface. This change in pressure with time is expressed as:

$$\frac{dP_g}{dt} = \frac{R_g}{V}\left[N\frac{dT}{dt} + T\frac{dN}{dt} - \frac{3NT}{R}\frac{dR}{dt}\right] \tag{12}$$

where R_g is the gas constant and N is the number of moles of volatiles inside the bubble at any given time. The flow of mass through the bubble-polymer interface dN/dt is related by Fick's first law as:

$$\frac{dN}{dt} = \frac{4\pi R^2 \rho D}{M}\frac{\partial C}{\partial r}\bigg|_R \tag{13}$$

where M is the molecular weight of the diffusant. The differential $\partial C / \partial r|_R$ refers to the concentration gradient at the interface, obtained from the numerical solution of Equation (3).

Table 1. Kinetic parameters for the chemical reactions in poly(amic acid) precursors.

	Amidation	Imidization
Apparent order of reaction	n = 1	n = 2
Heat of reaction	41.06 J/g	125.90 J/g
Frequency factor	5.61×10^{14} min^{-1} (9.34×10^{12} s^{-1})	3.21×10^{17} L·mol^{-1}·min^{-1} (5.35×10^{15} L·mol^{-1}·s^{-1}).
Activation Energy	104.60 kJ/mol	148.50 kJ/mol

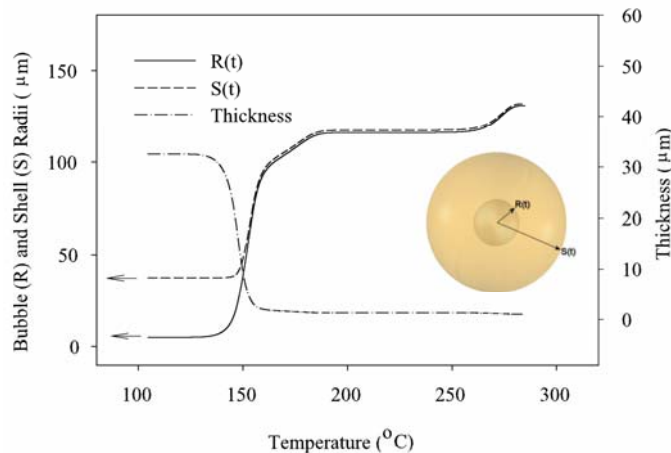

Figure 3 Inflation of a spherical particle of 75μm. Heating rate = 100°C/min, BA content = 0.05 weight fraction. Initial nucleus radius (R_0) = 5 μm.

Equations 3, 4, 11 and 12 comprise the set of governing equations for the growth of the spherical precursor particle containing a concentric spherical nucleus.

Parametric analysis of morphological development during particle inflation

As described earlier, the growth of the bubble is considered to begin at the moment that the process temperature reaches the precursor's effective T_g. At this point the bubble grows until increased viscosity due to molecular changes and solvent desorption restricts further growth. The simulated behavior of bubble growth for a spherical particle with a central spherical nucleus is presented in Figure 3. The growth process is fast initially, but tapers off into a plateau as viscosity increases. The observed trend can change depending on different parameter combinations. For example, Figure 3 shows a deceleration in the growth rate followed by a short linear increase and eventually the complete cessation of growth. Such prediction is explained as a momentary increase in viscosity in the vicinity of the growing front due to the concentration decrease in the interface as primary blowing agent is depleted and secondary blowing agent is produced. Figure 4 shows a superposition of both the growth profile and the viscosity of the precursor at the interface where this viscosity fluctuation can be seen.
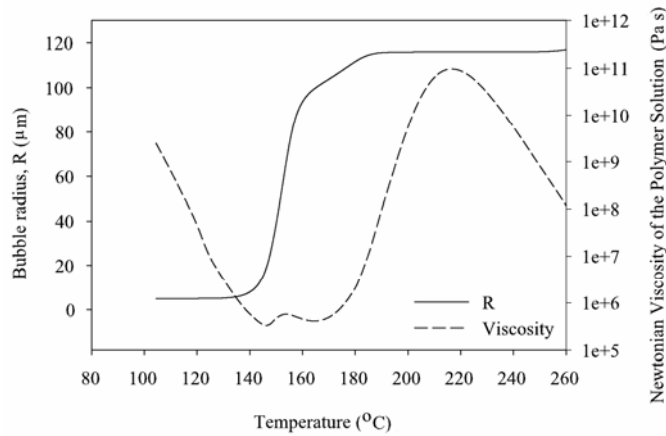

Figure 4 Viscosity of the precursor and bubble radius during the inflation process.
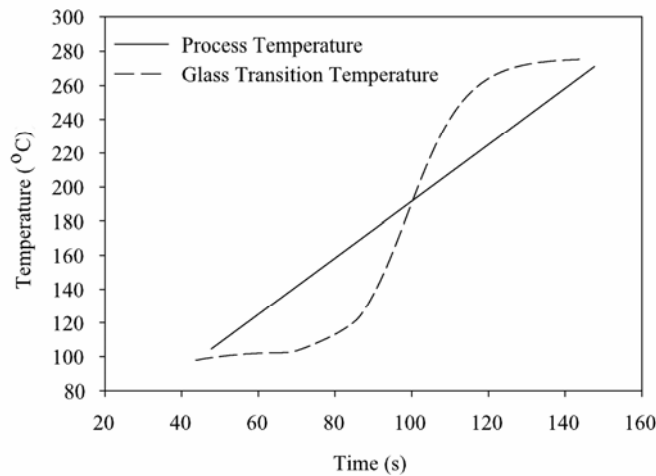

Figure 5 Process and glass transition temperatures of a PAA precursor particle
undergoing inflation at 100 °C/min

Material and transport properties such as viscosity and diffusivity are strongly related to the T_g of the precursor solution. Figure 5 shows the changes in T_g that the precursor goes through during inflation as solvent desorbs from the particle and condensation reactions take place. The T_g changes from values close to that of the pure poly(amic acid) (i.e. 110°C) to that of the pure polyimide (i.e. 276°C). Comparison of the profile for process and glass transition temperatures versus time and the bubble growth profile shows that there is a strong correlation between the differences between T and T_g at any time and the growth behavior (Figure 6). The gray area highlights the range where inflation occurs in the present example.
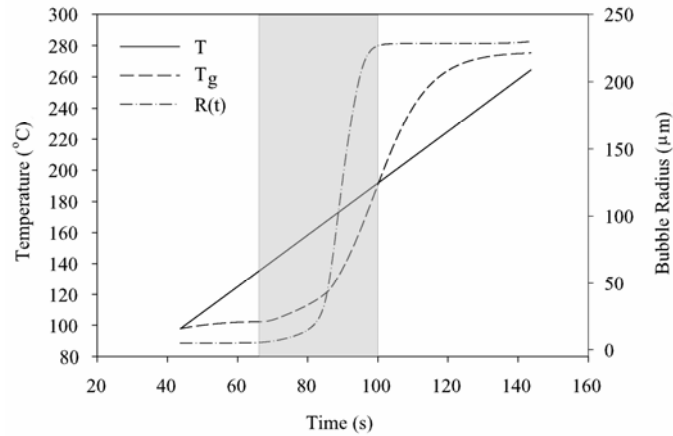

Figure 6 Bubble radius (R), process (T) and glass transition (T_g) temperatures. Gray area highlights the range where inflation occurs.
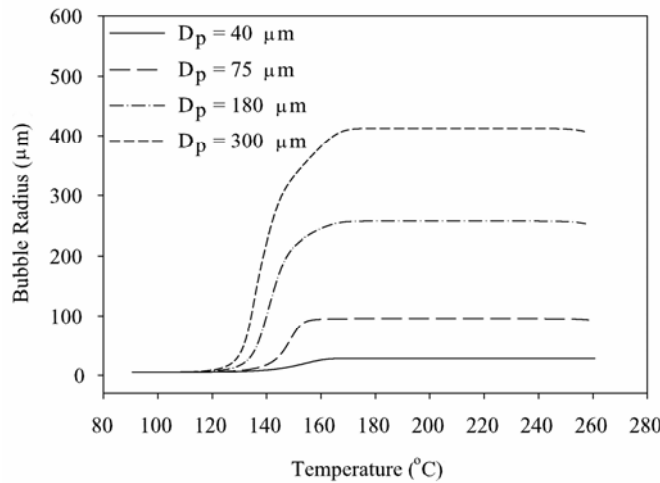

Figure 7 Inflation curves for spherical bubbles inside particles of different sizes. Heating rate (25°C/min) nucleus size (R_0=5µm) and initial BA content (0.15 wt. fr.) constant.

Effect of particle size

Earlier experimental observations [2, 3] had shown that inflation of smaller particles was restricted due to increased external desorption prior to inflation. Such behavior is accurately depicted by the model as shown in Figure 7. Smaller particles appear to have a lower inflation in general. Although such behavior is partly expected

due to the lower amount of polymer present, this reduced inflation also responds to the fact that smaller particles have a higher specific surface (i.e. ratio of surface area to volume) and therefore allow a higher pre-inflation desorption of blowing agent which limits its growth.
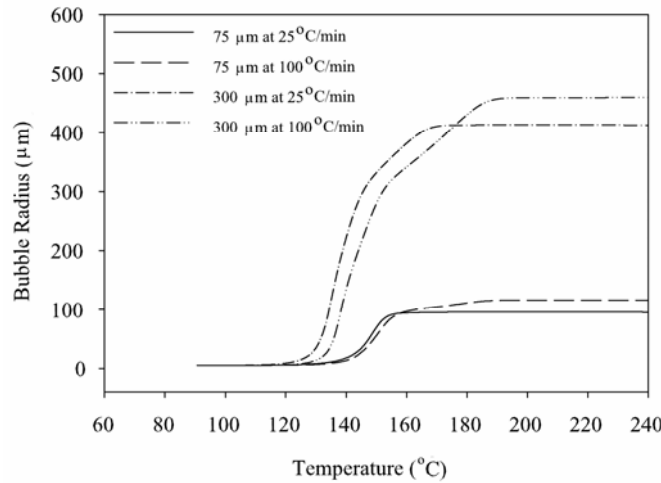

Figure 8 Inflation curves for spherical bubbles inside particles of 75 and 300 μm subjected to different heating rates.
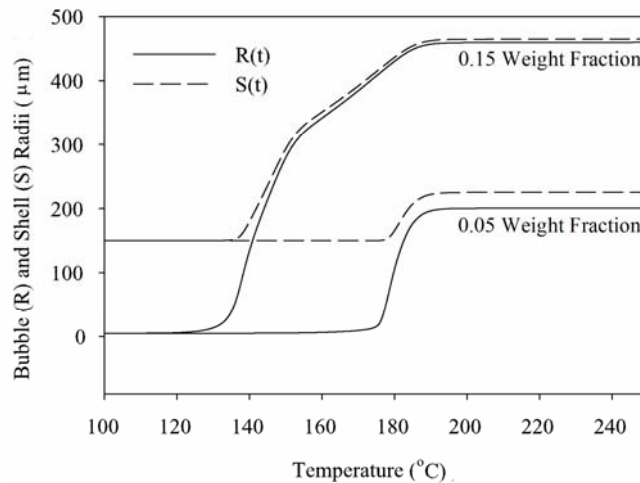

Figure 9 Inflation of spherical particles with different primary BA contents. Heating rate of 100 °C/min and particle size of 300 μm

Effect of heating rate

Experimental observations on the growth behavior of particles subjected to different heating rates showed that lower heating produced in general simpler microstructures [2]. Simulation of inflation under different rates shows that slower heating rates develop into smaller microspheres (Figure 8). In a similar way as with a decrease in particle size, a slower heating rate allows for more homogeneity in terms of concentration and temperature, as well as faster depletion of volatiles throughout the particle. As a consequence of the homogeneity in the particle, it can be seen that the change in growth rate due to viscosity fluctuations mentioned earlier tends to disappear in smaller particles and at slower heating rates. On the other hand a faster heating rate creates a larger temperature lag within the particles therefore delaying the onset of inflation (Figure 8).

Effect of primary blowing agent concentration

Simulation of particle growth at 100°C/min for 300 μm particles with different blowing agent contents is presented in Figure 9. As it can be expected, particles with higher blowing agent content show a higher inflation. Lower concentrations produce microstructures with a thicker shell due to incomplete inflation. Precursor plastization is evident in the lower inflation onset of particles with higher blowing agent content.

Effect of nucleus size

From previous analysis during the stages prior to particle inflation [4, 5], it was found that nucleus size is a determinant parameter in the growth of potential nuclei. Such analysis showed that in general, particles above 2 μm would achieve inflation regardless of the conditions. Based on these results, the simulation of thermal treatment for large particles (300μm) with large volatile content (0.15 wt. fr.) under high heating rates would be expected to yield inflation. This indeed is the case as can be evidence in Figure 10. However, upon varying the size of the initial nucleus it has been found that although all particles indeed exhibit bubble growth, small nuclei (R_0 = 0.5μm) only exhibited 0.4μm of radial growth increasing to a bubble of only 1.8μm in diameter (too small to be visible in the scale of Figure 10). Particles containing larger nuclei (5 and 25μm) develop successfully into microstructures showing different inflation onsets, but a similar final growth. The change in nuclei dimensions above 5μm does not appear to change substantially the morphological development of spherical particles.
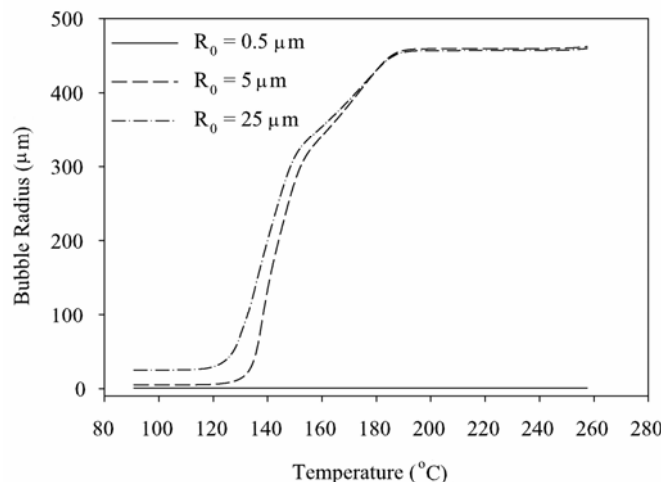

Figure 10 Bubble radius (R) for spherical microstructures (300 μm) with different initial nucleus sizes (Ro). Heating rate of 100 °C/min, BA content of 0.15 wt. fr.

Conclusions

The present paper presents a first principles numerical approach for the simulation and understanding of the powder foaming process. Spherical particles with concentric spherical nuclei are assumed as the studied geometry. The governing transport equations are solved in an iterative fashion by updating the materials and transport properties of the precursor. This provides an accurate representation of the system at any moment during the simulation.

A parametric study was performed on the numerical analysis and experimental observations were corroborated. Additionally new phenomenological information not observed preciously during experiments was evidenced. Several parameters were found to influence the particle growth by allowing or restricting the availability of volatile blowing agent to the developing bubble. It was found that parameter combinations that allow large concentration

gradients in the vicinity of the growing bubble can affect the growth rate of the bubble. In these cases, a sharp decrease in bubble growth rate is observed at the apex of the growth regime and is believed to respond to interfacial viscosity fluctuations. While this study focuses primarily on spherical particle geometries containing concentric nuclei, the results provide a framework for the future understanding of inflation of precursor particles containing multiple nuclei and complex geometries.

References

1. Weiser, E.S., Johnson, T.F., St. Clair, T.L. and Echigo, Y., *High Perform. Polym.*, <u>12,</u> 1-12. (2000).
2. Cano, C.I., Weiser, E.S. and Pipes, R.B., *Cell. Polym.*, <u>23</u>, 299 (2004).
3. Cano, C.I.,Weiser, E.S., Kyu, T. and Pipes, R.B., *Polymer*, <u>46</u>, 9296 (2005).
4. Cano, C.I., Ph.D. Dissertation, Dept. of Polymer Engineering, The University of Akron, (2005).
5. Cano, C.I., Kyu, T. and Pipes, R.B., *Polym. Eng. Sci.*, under review.
6. Kim, S. I., Pyo, S. M. and Ree, M. *Polymer*, <u>39</u>, 6489 (1998).
7. Arefmanesh, A., Advani, S.G. and Michaelides, E.E., *J. Heat Mass Transfer*, <u>35</u>, 1711 (1992).